

Monte Carlo simulation of the $S = \frac{1}{2}$ antiferromagnetic Heisenberg chain and the long-distance behavior of the spin-correlation function

Kenn Kubo*

*Center for Fundamental Materials Research and Department of Physics and Astronomy,
Michigan State University, East Lansing, Michigan 48824*

T. A. Kaplan

*Department of Physics and Astronomy and Center for Fundamental Materials Research,
Michigan State University, East Lansing, Michigan 48824*

J. R. Borysowicz

Department of Physics and Astronomy, Michigan State University, East Lansing, Michigan 48824
(Received 31 May 1988)

We present a new Monte Carlo simulation of the correlation function $C(r)$ between two spins separated by a distance r in the ground state of the spin- $\frac{1}{2}$ Heisenberg chain. The calculation is based on the Sutherland mapping between the spin-chain ground state and the six-vertex model at its critical temperature. New results are obtained for rings with the number of spins $N = 32$ and 40. We give evidence that the asymptotic decay of $C(r)$ at large r is slower than the $1/r$ behavior of Luther and Peschel, and that this might be attributed to a logarithmic factor, i.e., $C(r) \sim (A/r)(\ln r/r_0)^\sigma$, with $\sigma \approx 0.2$ to 0.3.

I. INTRODUCTION

One-dimensional spin chains have been attracting considerable attention in many-body and condensed matter physics for a long time.¹ In recent years especially intensive investigations have been made in this field stimulated by Haldane's conjecture,² which claims the existence of an energy gap between the ground state and the excited states of the Heisenberg antiferromagnet with integer spins. Rigorous analytical solutions are available only for the $S = \frac{1}{2}$ XYZ model³ and recently found solvable models with higher-order interactions for $S \geq 1$.⁴ Even in the case of rigorously solved models quantities such as spin-correlation functions are not easily found rigorously and one must rely on numerical methods or some approximate method.⁵ As far as critical properties field theoretical methods are quite powerful and lead to important results.^{5,6} Their arguments usually include several assumptions which are plausible though not proved. Therefore numerical investigation is necessary to check their validity. Quite a few numerical methods are known so far and have been used to study the spin correlation functions of one-dimensional spin chains. We discuss some of them here to compare a new method we propose and apply in this paper.

The exact diagonalization of small chains⁷ is the most reliable method as it includes no approximation or statistical errors necessarily accompanying stochastic methods. On the other hand, the system size treated is rather restricted (to date, $N \leq 24$ for $S = \frac{1}{2}$, $N \leq 16$ for $S = 1$, and $N \leq 12$ for $S = \frac{3}{2}$) and the extrapolation process to infinite chains is quite important. One of the well-known extrapolation schemes is the $1/N^2$ fit used in the

famous Bonner and Fisher⁷ work. Recently the finite-size scaling idea was used to extract critical behaviors in a variety of problems quite successfully.⁸ In some cases, however, the available system size turns out still not large enough even with use of finite-size scaling. Quite recently the idea of conformal invariance was found to be very useful.⁹ The transfer-matrix method based on the Trotter formula was applied to the XXZ model with $S = \frac{1}{2}$, 1, and $\frac{3}{2}$ for estimation of the critical indices.¹⁰ In this method the system size has practically no restriction. On the other hand, the available number of Trotter slicings N_t is rather small and an extrapolation procedure to infinite N_t was employed. The critical indices obtained showed good agreement with previous analytical results for $S = \frac{1}{2}$ in a region close to the XY model but the results were not good in regions close to the isotropic models, where the N_t employed seemed not large enough. Monte Carlo simulation based on the Trotter formula is becoming a standard method to study quantum-mechanical many-body systems;¹¹ its applicability is quite general and furthermore rather large systems can be treated. Extrapolation to infinite N_t is again necessary. At high temperature one can treat N_t large enough to be practically infinite. More and more Trotter slicings are necessary with decreasing temperature. Two limiting processes are necessary to obtain ground-state properties, namely to infinite N_t and to $T=0$, which makes it difficult to apply this method to ground-state properties. This seems to be the reason why no accurate analysis of ground-state critical behavior by this method has been reported. Careful treatment of these two limiting processes would show the usefulness of this method for ground-state properties.

The MC simulation we investigate here has quite limit-

ed applicability, i.e., to ground-state properties of the $S=\frac{1}{2}$ XYZ model. On the other hand, it has a merit that only one limiting process is necessary. Of course extrapolation to the infinite system is necessary, as with the Trotter approach. But reasonably large systems could be simulated. The method is based on the equivalence of the ground state of the $S=\frac{1}{2}$ XYZ model and the maximum-eigenvalue eigenvector of the transfer matrix of the eight-vertex model.¹² We apply the method to calculate the ground-state spin correlations of the antiferromagnetic Heisenberg model. A preliminary account of this work has been presented.¹³

Recently another MC calculation of this model has been carried out.¹⁴ This is an early version of the Green's function Monte Carlo (GFMC) method.¹⁵ It shares with the Sutherland mapping approach the advantage of being directly a ground-state calculation (so the $T \rightarrow 0$ extrapolation is unnecessary). The accuracy of the method is limited by the accuracy of the variational wave function which is used in importance sampling, and there is a difficulty in going to very large systems associated with the need to estimate the second-order correction to the importance sampling. The structure factor at wave vector π is calculated in Ref. 14 for up to 110 spins.

We shall use the results of the present MC calculation plus the known exact results⁷ to address the question of the asymptotic behavior of the spin-correlation function $C(r, N)$ [see Eq. (2)]. In particular we shall present evidence which suggests that the asymptotic decay of $C(r, \infty)$ as $r \rightarrow \infty$ is slower than that of Luther and Peschel⁵ (LP), and we shall argue that this might be attributed to a logarithmic term multiplying the $1/r$ behavior of LP, namely, $C(r, \infty) \cong A(\ln r / r_0)^\sigma / r$ for large r , with $\sigma \cong 0.2$ to 0.3 .

II. MODELS

In this section we explain briefly the $S=\frac{1}{2}$ XYZ model and the eight-vertex model, and introduce notations.

A. XYZ model

The $S=\frac{1}{2}$ XYZ model is described by the Hamiltonian

$$H_{XYZ} = -J \sum_i [(1 + \Gamma) S_i^x S_{i+1}^x + (1 - \Gamma) S_i^y S_{i+1}^y + \Delta S_i^z S_{i+1}^z], \quad (1)$$

where S_i^α denotes the α component of a spin- $\frac{1}{2}$ particle at site i . We consider the case with $J > 0$ and $1 \geq \Gamma \geq 0$. This parameter region proves to be general if one uses cyclic exchanges of notation of S_i^x , S_i^y , and S_i^z and rotations of every other spin about the z axis. Basis vectors which diagonalize the z component of the spin at each site are used throughout the following discussions. We notice that off-diagonal matrix elements of the Hamiltonian in this representation are seminegative definite. The XXZ model is the version with $\Gamma = 0$ and includes all the well-known cases, i.e., ferromagnetic Heisenberg model ($\Delta = 1$), antiferromagnetic Heisenberg model ($\Delta = -1$), and XY model ($\Delta = 0$). This model conserves S^z , the z component of total spin. We are interested in the

ground-state correlation function

$$C(r, N) = 4(-1)^r \langle \Psi_N | S_i^z S_{i+r}^z | \Psi_N \rangle, \quad (2)$$

where Ψ_N denotes the ground-state wave function of a ring with N spins. The structure factor at wave vector π

$$S(N) = 1 + 2 \sum_{r=1}^{N/2-1} C(r, N) + C(N/2, N) \quad (3)$$

is a quantity of interest for the antiferromagnetic Heisenberg model.

B. Eight-vertex model

The eight-vertex model is a classical model on a square lattice. An arrow is placed on each bond connecting nearest-neighbor sites and an energy assigned to each configuration of four arrows about a vertex. Among the 16 possible vertex configurations only the eight with an even number of incoming or outgoing arrows are allowed. Statistical weights for these configurations are given in Fig. 1. Now we consider a square lattice with M rows and N columns with periodic boundary conditions (N and M are even). The partition function of the system is given by

$$Z_{N \times M} = \text{Tr}(T_N)^M, \quad (4)$$

where T_N is the transfer matrix between the successive rows. We use the variable $\sigma_{ij} = 1(-1)$ to represent the up (down) arrow on the vertical bond connecting sites (i, j) and $(i, j + 1)$ and similarly $\tau_{ij} = 1(-1)$ to represent the arrow pointed to the right (left) on the horizontal bond between (i, j) and $(i + 1, j)$. Then a configuration of vertical arrows in a row is represented by $(\sigma_1, \sigma_2, \dots, \sigma_N)$ where $\sigma_i = \pm 1$ and therefore T_N may be regarded as an operator in the same vector space of the Hamiltonian of a spin chain with N spins. The correlation of vertical arrows on the same row on a $N \times M$ lattice $C(r, N; M)$ is defined as

$$C(r, N; M) = (-1)^r \langle \sigma_{ij} \sigma_{i+r, j} \rangle_{N \times M} \quad (5)$$

and written with use of T_N as

$$C(r, N; M) = (-1)^r \text{Tr}[\sigma_i^z \sigma_{i+r}^z (T_N)^M] / Z_{N \times M}, \quad (6)$$

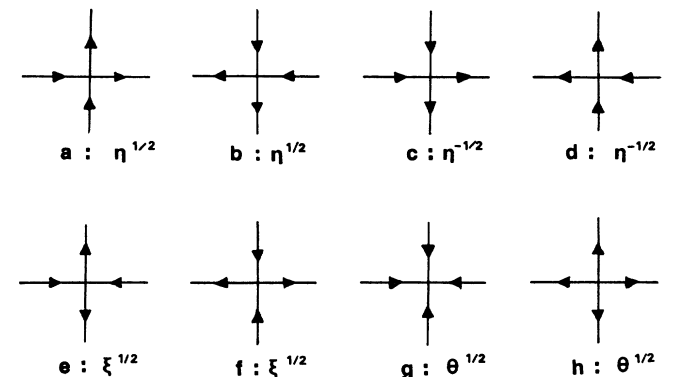


FIG. 1. Allowed vertex configurations and their statistical weights of the eight-vertex model. The last two are prohibited in the six-vertex model.

where σ_i^z is a Pauli matrix on site i . The six-vertex model is a version where the last two configurations in Fig. 1 are prohibited, i.e., $\theta=0$. In this model $\Sigma = \sum_i \sigma_{ij}$ is independent of j and correspondingly T_N conserves S^z . Also $\Pi = \sum_j \tau_{ij}$ is a conserved quantity.

III. SUTHERLAND'S MAPPING THEOREM

Sutherland proved that the transfer matrix T_N of the eight-vertex model commutes with the XYZ Hamiltonian of N spins with periodic boundary conditions if

$$2\Delta = \eta + \eta^{-1} - \xi - \theta \quad (7a)$$

and

$$\Gamma = (\xi\theta)^{1/2}. \quad (7b)$$

Then seminegative definiteness of the off-diagonal matrix elements of H_{XYZ} and the semipositive definiteness of those of T_N lead to the equivalence of the ground state of H_{XYZ} and the eigenstate of T_N with the maximum eigenvalue (with help of the famous Frobenius' theorem). Another condition is necessary to apply this theorem, i.e., the whole space must be connected both by T_N and H_{XYZ} . It is easily seen that H_{XXZ} and T_N of the six-vertex model connect by successive operations all the states in each subspace with a fixed S^z . Therefore equivalence holds in each subspace with given $S^z = \Sigma/2$ between the XXZ model and the six-vertex model, if $2\Delta = \eta + \eta^{-1} - \xi$ and $\theta=0$. For $\Gamma > 0$ we can write down the XYZ Hamiltonian as

$$H_{XYZ} = H_{XXZ} + H' \left[H' = -J\Gamma \sum_i (S_i^+ S_{i+1}^+ + S_i^- S_{i+1}^-) \right]$$

and H' changes S^z by ± 2 . Also T_N of the eight-vertex model with $\theta > 0$ changes S^z by a multiple of 2, i.e., the difference of Σ between adjacent two rows is a multiple of 4. This is a result of the periodic boundary condition which imposes $n_e + n_g = n_f + n_h$ on each row for the numbers $n_e, n_g, n_f,$ and n_h of vertex $e, g, f,$ and h on the row [$\delta\Sigma = 2(n_e + n_h - n_f - n_g)$]. Therefore the whole space is divided into two subspaces with even or odd S^z and the equivalence holds in each subspace. As the state with the maximum eigenvalue dominates Eqs. (4) and (6) in the limit $M \rightarrow \infty$, the correlation function (2) is given by

$$C(r, N) = \lim_{M \rightarrow \infty} C(r, N; M). \quad (8)$$

This mapping is useful for obtaining the ground-state spin correlation of the XYZ model, as the classical statistical average $C(r, N; M)$ can be calculated easily with the help of MC simulations. In the case of the XXZ model, the average over configurations in the six-vertex model with a fixed value of $\Sigma = 2S^z$ is sufficient where S^z is the total spin of the ground state.

In the following we apply this method to the antiferromagnetic Heisenberg model ($\Delta = -1, \Gamma = 0$). Although some freedom still remains in the choice of η and ξ , we use the values which give the same weights for vertices a and c in Fig. 1, i.e., $\eta = 1$ and $\xi = 4$.

IV. MONTE CARLO SIMULATION OF THE SIX-VERTEX MODEL

In this section we explain the MC technique for the six-vertex model. The checker board lattice mapped from the XXZ model through the Trotter formula is equivalent to the eight- or six-vertex model and MC studies on that lattice have been reported by several authors.^{16,17} Their calculational techniques, and ours, are essentially the same (although their fundamental approach is essentially different from ours, as explained in the introduction).

In a MC simulation we generate configurations of arrows updating successively the initial configuration in stochastic ways. For an Ising lattice updating is simply done flipping one spin at each site. Flipping a single arrow is not allowed on the eight-vertex model as it causes prohibited configurations of vertices (see Fig. 2). One immediately sees that possible updating processes are to flip all arrows to the opposite direction on closed loops, since an even number of arrows about each vertex must be flipped. This process is always allowed on the eight-vertex model but it is allowed on the six-vertex model only when all the arrows are pointed in the same way along the loop. The minimum loop is a square of four bonds and we call flipping along it a minimum local flip (MLF). It can be shown that MLF's on all possible squares connect all the configurations in a subspace with a given Σ and Π , provided $\Sigma \neq \pm N$ and $\Pi \neq \pm M$ (see the Appendix). A flip is called global if the loop stretches from one boundary to another, i.e., the winding number¹⁶ is > 0 . Global flips on the loops which have winding number equal to 1 in the horizontal direction (HGF) connect subspaces with different values of Π and those in the vertical direction (VGF) connect subspaces with different values of Σ . We do not need VGFs as we can restrict configurations to the $\Sigma = 0$ subspace: The ground state of the antiferromagnetic Heisenberg model is known to be a singlet.¹⁸ To obtain the statistical average corresponding to Eq. (5) in the $\Sigma = 0$ subspace we need HGF's. As HGF's we employ those which flip all the horizontal ar-

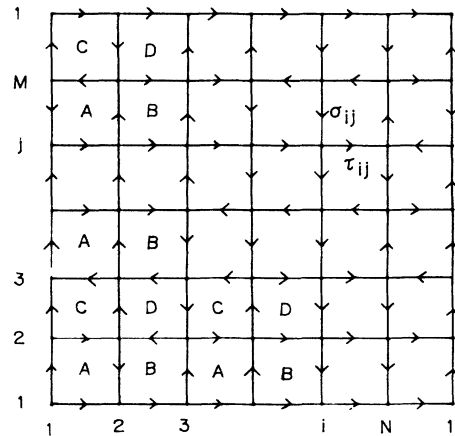


FIG. 2. An example of the configurations of the eight-vertex model on the $N \times M$ square lattice. A division of the sublattices in the MC simulation is illustrated.

rows on a given row (assuming of course that they are all parallel). Both MLF's and HGF's on all the rows compose an ergodic updating process.

Next we choose the transition probabilities which give the correct equilibrium ensemble of MC steps, i.e., the detailed balance condition is required for the transition probability for a elementary flipping process. We apply the heatbath method; a flipping process is accepted if $R < W_n / (W_n + W_o)$ where W_n and W_o are weights for new and old configurations and R is a random variable generated between zero and unity. The total lattice is divided into four sublattices ($A-D$) on each of which probabilities for LMF's are all independent (Fig. 2). Also HGF's on even (odd) rows occur independently. The unit MC step is, for example, the total of processes of LMF's on sublattice A , LMF's on B , LMF's on C , LMF's on D , HGF's on even rows, HGF's on odd rows, and those processes in the reversed order. In each subprocess squares or rows are visited once in a fixed order. Taking this unit MC step we can easily prove the detailed balance condition of the transition probability. We sample data twice in a unit MC step, in the middle and at the end. So doubling the unit MC step has practically no disadvantage. Correlations between σ_{ij} and $\sigma_{i+r,j}$ are measured for all i and j and averaged at each MC step to give $C(r, N; M)$.

We simply chose HGF's on rows. As the probability for a row to have all arrows on it parallel decreases exponentially with increasing N , the acceptance of HGF's becomes negligible for large N . To have appreciable acceptance of HGF's we have to search for the loops with all arrows aligned along it. Such a method was studied by Cullen and Landau¹⁷ in a MC simulation of a checker-board lattice. As far as we understand, however, it was quite time consuming and a good algorithm for the process is not known. As will be shown in the next section it turns out that HGF's are not really necessary to get the quantum-mechanical expectation values and we employed only MLF's in the simulations for $N \geq 24$.

V. EXTRAPOLATION TO INFINITE M

From Eq. (7) we immediately see that the finite- M effect decreases exponentially, namely

$$\delta C(r, N; M) = C(r, N; M) - C(r, N) \sim (\lambda_1 / \lambda_0)^M (-1)^r [\langle 1 | \sigma_i^z \sigma_{i+r}^z | 1 \rangle - \langle 0 | \sigma_i^z \sigma_{i+r}^z | 0 \rangle], \quad (9)$$

where λ_0 and λ_1 are the largest and the second largest eigenvalues of T_N . The ratio λ_1 / λ_0 is expected to approach unity as $N \rightarrow \infty$. If it goes as λ_1 / λ_0

$\sim 1 + O(1/N)$, then $\ln(\lambda_1 / \lambda_0)^M$ will be linear in M/N and this is found by numerical transfer-matrix calculations for $N=4-8$ as shown in Fig. 3. Also additional N dependence is seen to be weak. MC simulations also have been performed for $N=6$ and 12 with $M/N=1, 2, 3$, and 4 for $N=6$ and $M/N=1, 2, 2.5, 3$, and 4 for $N=12$. The average was taken over 1.2×10^5 MC steps for $N=6$ and 8×10^4 steps for $N=12$. Some of the results are shown in Fig. 4 together with the exact transfer-matrix results (\cdot) for $N=6$. Data of $C(r, N; M)$ are extrapolated assuming $C(r, N; M) = C(r, N) + ab^{M/N}$ by using the least-square fit. The result is shown in Table I. We see that the estimated values of $C(r, N)$ are within a half-percent error. The errors estimated from the least-square fit are too small compared to the deviation of the extrapolated values from the exact ones for $N=12$. This means our MC run was not long enough to average out fluctuations with a long decay time. These fluctuations we think are due to fluctuations of Π , which last long due to the low acceptance of HGF's. The acceptance of HGF's decreases very rapidly with increase of N . We had 0.017 per row acceptances of HGF's per MC step for $N=6$ but the number decreases to 1.5×10^{-4} for $N=12$, while 0.32 per site acceptance for MLF's occurs independently of N . No acceptance of a HGF occurred during 8×10^4 steps for $N=24$. This fact means that we need a different algorithm for HGF's to obtain the correct $C(r, N; M)$ for large N . However, we are only interested in the quantity $C(r, N)$, not $C(r, N; M)$ itself. So we look for another quantity which gives $C(r, N)$ in the limit $M \rightarrow \infty$ and can be obtained more easily.

Dividing the summation over the whole configuration into summations in subspaces with fixed value of Π we write

$$C(r, N; M) = \sum_{\Pi} P(\Pi) C^{(\Pi)}(r, N; M), \quad (10)$$

where $P(\Pi)$ is the probability distribution for Π and $C^{(\Pi)}(r, N; M)$ is the average in the subspace. As M increases the distribution $P(\Pi)$ becomes peaked around its mean value Π_0 as

$$P(\Pi) \simeq \exp[-(\Pi - \Pi_0)^2 / 2\zeta], \quad (11)$$

with $\zeta = \langle (\Pi - \Pi_0)^2 \rangle$ proportional to M . Then we rewrite Eq. (11) as

$$C(r, N; M) \simeq C^{(\Pi_0)}(r, N; M) + \frac{1}{2} \frac{\partial^2}{\partial \Pi^2} C^{(\Pi)}(r, N; M) \Big|_{\Pi = \Pi_0} \zeta \quad (12)$$

replacing summation by integration. As the second term

TABLE I. Correlation function $C(r, N)$ and the structure factor $S(N)$, resulting from MC simulations with HGF's. The number in parentheses is the error in the last decimal place. Extrapolation assuming exponential dependence on M was used. Exact values obtained by numerical diagonalization (Ref. 7) are added for comparison.

N		$C(1, N)$	$C(2, N)$	$C(3, N)$	$C(4, N)$	$C(5, N)$	$C(6, N)$	$S(N)$
6	exact	0.622 84	0.277 35	0.309 02				3.109 40
6	MC	0.622 5(3)	0.276 7(5)	0.308 5(4)				3.107 (2)
12	exact	0.598 60	0.250 44	0.221 10	0.161 14	0.163 21	0.142 65	3.931 63
12	MC	0.598 9(2)	0.251 1(4)	0.222 1(5)	0.162 3(5)	0.164 1(6)	0.143 5(6)	3.941 (5)

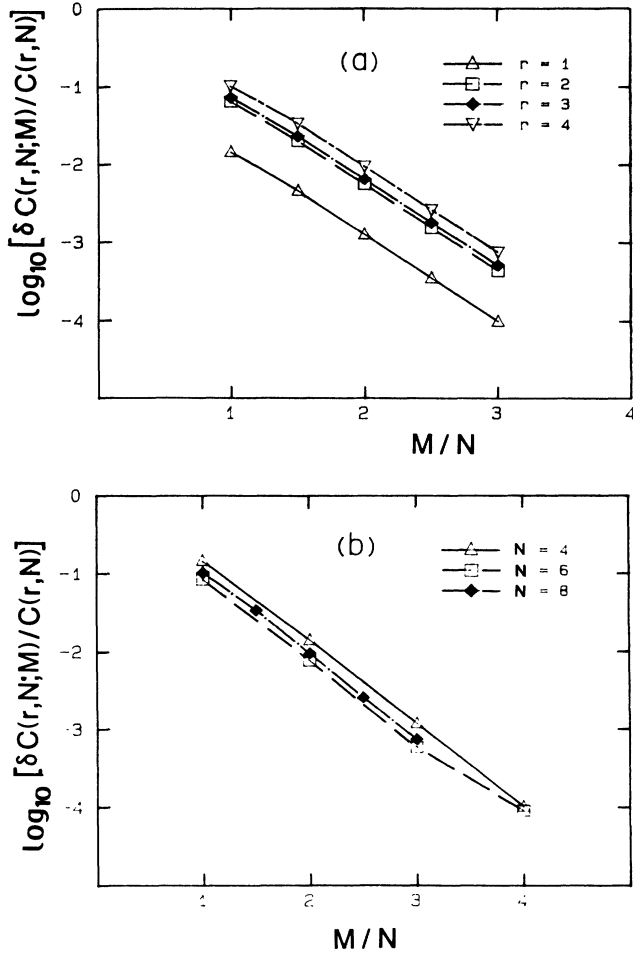


FIG. 3. $\log_{10}[[C(r,N;M)-C(r,N)]/C(r,N)]$ obtained with use of the transfer matrix is plotted against M/N . (a) Plots for different r for $N=8$. All the plots show the same exponent consistent with (9). (b) Plots of correlations between spins with the largest distance for different chains ($N=4-8$). They show only a weak- N dependence.

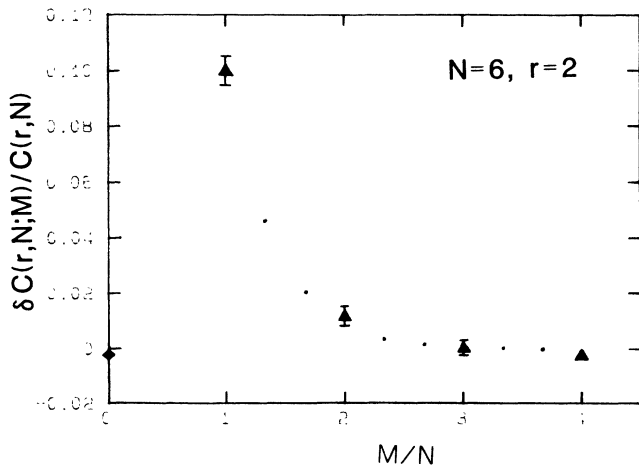


FIG. 4. M dependence of $[C(2,6;M)-C(2,6)]/C(2,6)$ obtained by the MC simulation with HGF. Dots (\cdot) are the exact transfer-matrix results. The estimate of $C(2,6)$ with use of the least-square fit assuming an exponential dependence on M/N is depicted by \blacklozenge on the vertical axis.

is $O(1/M)$ as $M \rightarrow \infty$, we have

$$\begin{aligned} \delta C^{(\Pi_0)}(r,N;M) &= C^{(\Pi_0)}(r,N;M) - C(r,N) \\ &= O(1/M), \end{aligned} \tag{13}$$

for large M . As the MC simulation with only MLF's gives the statistical average in a subspace with fixed Π , $C^{(\Pi_0)}(r,N;M)$ is easily obtained if we know Π_0 . In our case $\Pi_0=0$ is easily deduced from symmetry.

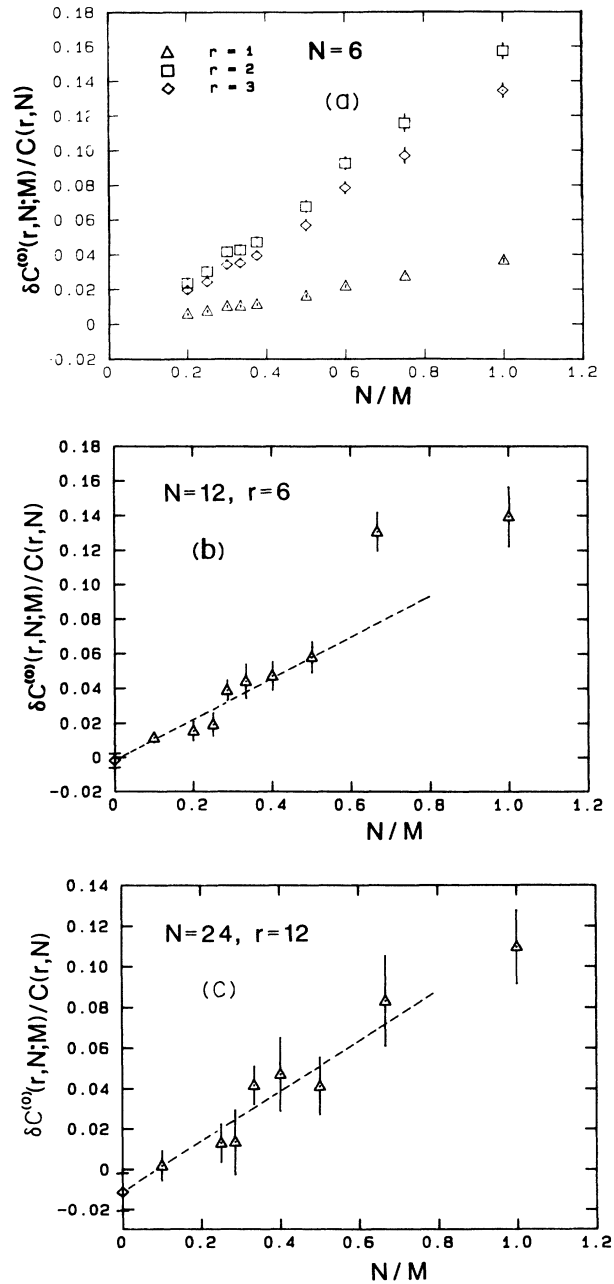


FIG. 5. M dependence of $[C^{(0)}(r,N;M)-C(r,N)]/C(r,N)$ obtained by the MC simulations without HGF: (a) $N=6$, $r=1, 2$, and 3 ; (b) $N=12$, $r=6$; (c) $N=24$, $r=12$. Best fits which assume linear dependence on M^{-1} are depicted in (b) and (c) as dashed lines. Estimates of $C(r,N)$ are shown with their error bars on the vertical axis (\blacklozenge).

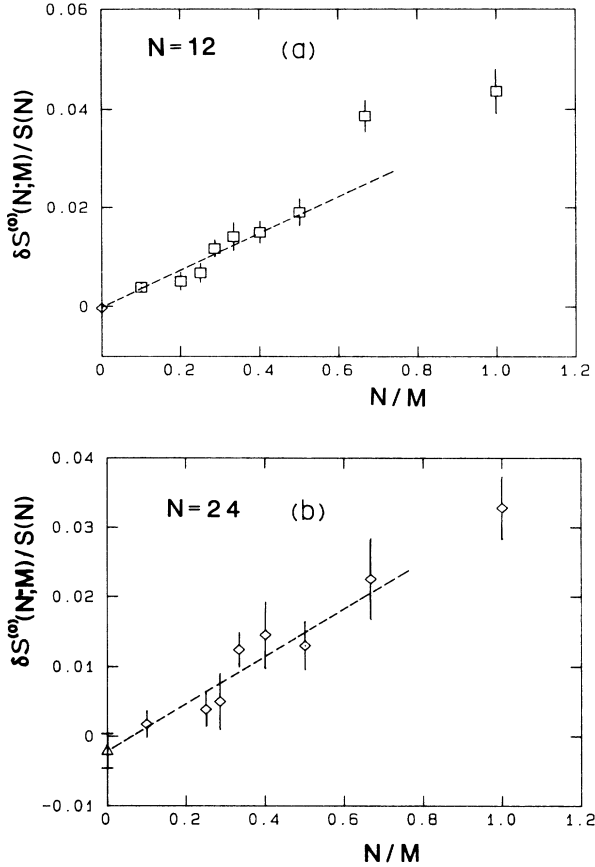


FIG. 6. M dependence of $[S^{(0)}(N;M) - S(N)]/S(N)$ obtained by the MC simulations without HGF. Estimates of $S(N)$ are also shown (\diamond for $N=12$, \triangle for $N=24$).

The approach of the MC data of $C^{(0)}(r,N;M)$ (note $\Pi_0=0$) to $C(r,N)$ is shown in Fig. 5 for $N=6, 12$, and 24 where the exact $C(r,N)$ is available. Linear dependence in M^{-1} is observed to hold rather nicely for large M ($M \geq 2N$), although deviation from the linearity is seen for intermediate value of M ($2N \geq M \geq N$). We estimated

$C(r,N)$ and the structure factor $S(N)$ using the least-squares fit of the data to an M^{-1} dependence for $M \geq 2N$ where the dependence is approximately obeyed in all the cases studied. One should also note that $\delta C^{(0)}(r,N;M)/C(r,N)$ is already fairly small at $M=2N$ for even $C(N/2,N)$ which is the correlation between the two farthest separated spins on the ring. The quantity is $\cong 0.06$ for $N=12$ and $\cong 0.04$ for $N=24$.

The finite- M effect on $S(N)$ decreases with increasing N as is shown in Fig. 6. We have observed small wiggling behavior around M^{-1} behavior whose real reason we do not understand. This wiggling is the main cause of the uncertainties of extrapolated values of $C(r,N)$ if we rely on data with not large enough M/N . This uncertainty may be reduced to less than 1% if we perform simulations up to $M=10N$ for $N \leq 24$. Extrapolated values of $C(r,N)$ and $S(N)$ are listed in Table II; they are in very good agreement with the exact values. A marked improvement over the results in Table I is seen for $N=12$, where we utilized data with $M \leq 10N$ for the extrapolation (we used data with $M \leq 5N$ for $N=6$).

The above result convinces us the method is quite useful for the calculation of $C(r,N)$. Computing time is about 4 h for 8×10^4 MC steps for $(N,M)=(24,240)$ on a CDC750. The increase of CPU time is proportional to NM for generating the ensemble and to N^2M for measurement of the correlation function. The CPU time for measurement is by no means negligible and amounts to 58% for $(N,M)=(40,400)$. The total CPU time increases proportionally to N^α with $\alpha=2-3$. We accomplished the simulation for $N=32$ and 40 where no numerical result for $C(r,N)$ ($r \geq 2$) has been reported. Data are obtained from the average over 8×10^4 MC steps for each M studied. Some of the results are shown in Fig. 7. The results show an upward curvature in M^{-1} ; it is not clear whether this is due to a fluctuational artifact or the real M dependence, as the statistical errors are fairly large compared to this curvature. The result of the extrapolation which assumed M^{-1} dependence for $M \geq 2N$ might be a little smaller in magnitude than the correct value if the curvature is real. The magnitude of the M dependence is,

TABLE II. $C(r,N)$ resulting from MC simulations without HGF's. Extrapolation assuming M^{-1} dependence was used. Exact values are taken from Ref. 7.

$r \setminus N$	6		12		24	
	MC	Exact	MC	Exact	MC	Exact
1	0.6223(5)	0.622 84	0.5985(2)	0.598 60	0.5927(2)	0.592 779
2	0.2761(10)	0.277 35	0.2504(4)	0.250 44	0.2445(3)	0.244 568
3	0.3076(10)	0.309 02	0.2210(5)	0.221 10	0.2055(4)	0.205 664
4			0.1610(5)	0.161 14	0.1434(4)	0.143 668
5			0.1631(6)	0.163 21	0.1315(5)	0.131 789
6			0.1424(6)	0.142 65	0.1062(6)	0.106 629
7					0.1019(6)	0.102 444
8					0.0886(7)	0.089 206
9					0.0880(7)	0.088 663
10					0.0802(7)	0.080 952
11					0.0821(7)	0.082 926
12					0.0776(8)	0.078 484
$S(N)$	3.104(4)	3.109 4	3.930(5)	3.931 63	4.807(12)	4.817 06

however, fairly small as one can see from Fig. 7; the relative difference between $C(16,32;64)$ and $C(16,32;320)$ is about 6% and that between $C(16,32;320)$ and $C(16,32)$ we expect less than 1%. Accordingly we can expect rather accurate results for the extrapolated data in spite of the simple M^{-1} dependence assumed.

The results of simulations for $N=40$ are shown in Fig. 8. In this case the data are accompanied with strong statistical fluctuations, which smear the M dependence of the data. We observe that the M dependence itself is again rather weak and we feel safe in using the simple M^{-1} extrapolation.

The results of extrapolation for $N=32$ and 40 are given in Table III. Comparison of the estimates of $C(1,32)$ and $C(1,40)$ with the exact values (obtained from the Bethe ansatz), i.e., 0.591 939 and 0.591 551, respectively, shows excellent agreement. We notice that the MC estimate of $C(1,32)$ [$C(1,40)$] gives a small negative (positive) deviation from the exact values although within the estimated errors.

We observed that the statistical fluctuations in our MC data for $C^{(0)}(r,N;M)$ at different r with the same N and M were strongly correlated. This correlation comes from the fact that in MC runs most of the configurations realized are composed of rather large clusters of antiferromagnetically ordered states of σ_{ij} , and thermal equilibrium is reached by domain wall motions rather than lo-

calized fluctuations. In such a situation subaverages of correlation functions (we have taken 4000 MC steps for a subaverage) for different r are strongly correlated and our final results still carry the effect. From the viewpoint of the correlation mentioned above it is highly probable that deviations of MC estimates of $C(r,N)$ from exact values have the same sign with that for $C(1,N)$. We expect therefore exact values of $C(r,N)$ to be larger than our estimates for $N=32$ and smaller for $N=40$ although within our estimated errors.

VI. EXTRAPOLATION TO INFINITE N

The bulk correlation function $C(r) \equiv C(r, \infty)$ and its decay at large r are of current interest and will be discussed in Sec. VII.

To obtain $C(r)$ we used a recently reported extrapolation method (Kaplan *et al.*⁸) based on the scaling relation

$$C(r,N) \simeq C(r)f(r/N) \quad (14)$$

for large r and N , where the scaling function $f(y)$ is determined numerically and given in the reference. In this method we extrapolate $C(r,N)/f(r/N)$ which, because $f(0)=1$, approaches $C(r)$ as $N \rightarrow \infty$. The extrapolation of $C(r,N)/f(r/N)$ rather than $C(r,N)$ leads to more accurate results since the variation of

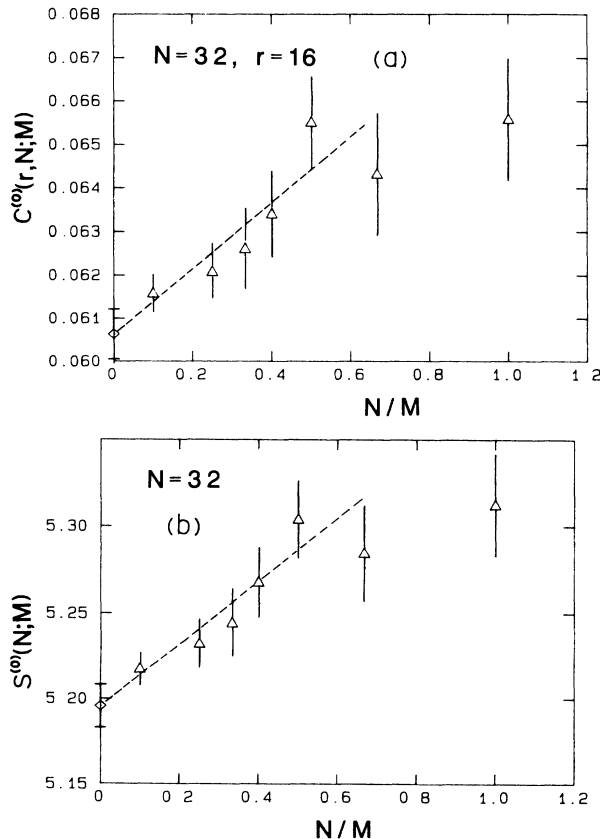


FIG. 7. (a) $C^{(0)}(16,32;M)$ and (b) $S^{(0)}(32;M)$. Best fits and estimates for $M = \infty$ are also shown.

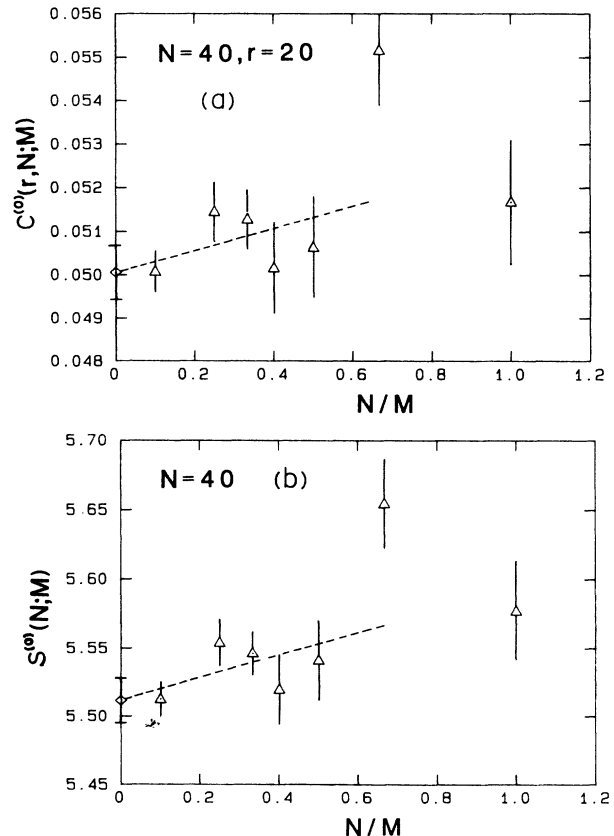


FIG. 8. (a) $C^{(0)}(20,40;M)$ and (b) $S^{(0)}(40;M)$. Best fits and estimates for $M = \infty$ are also shown.

$C(r, N)/f(r/N)$ with N is smaller than that of $C(r, N)$ alone, according to the scaling relation (14).

The extrapolated values of $C(r)$ are shown in Table III. For $r=1$ and 2, where the exact values are known,^{3,19} the agreement is excellent. For $r \leq 12$ we extrapolated the $C(r, N)$ known from the exact numerical calculations⁷ for N up to 24. The agreement with the results of Kaplan *et al.*,⁸ where only rings with $N \leq 18$ were used, is excellent. The errors reported here are reduced, as expected. The MC results for $N=32$ and 40 are consistent with $C(r)$. While their errors are too large to influence the extrapolation for the smaller r [where there are already many data, $C(r, N)$, $N=2r, \dots, 24$], they did influence the results for $r=11$ and 12; for $r > 12$ the determination of $C(r)$ is based essentially entirely on the MC results.

VII. LARGE- r BEHAVIOR OF $C(r)$

The question of how $C(r)$ approaches zero as $r \rightarrow \infty$ was investigated by Luther and Peschel⁵ (LP), who found, by analytical means, $C(r) \simeq A/r$ for large r . As pointed out later,^{6,20} LP neglected certain terms in the Hamiltonian, namely Umklapp terms in the framework of the fermion representation. These terms are far from negligible for the Heisenberg model and may modify the asymptotic behavior of $C(r)$. Previous studies based on exact calculations for finite systems ($N \leq 24$) (Ref. 7) did not investigate the modified asymptotic behavior in detail.²¹

It is rather widely believed that the Umklapp processes mentioned above will lead to some form of logarithmic corrections to the large- r behavior of $C(r)$.^{6,22} In this section we give a plausibility argument for a logarithmic dependence of the form

$$C(r) \simeq A \frac{(\ln r / r_0)^\sigma}{r}, \quad (15)$$

where A , σ , and r_0 are constants. We then present nu-

TABLE III. Correlation function $C(r, N)$. Columns labeled 32 and 40 are new MC results. The last column is the result of extrapolation from all available N values [4(2)24,32,40]. It should be remembered that the smallest N for given r is $2r$.

$r \setminus N$	32	40	∞
1	0.5919(1)	0.5916(1)	0.590 8(1)
2	0.2437(2)	0.2434(1.5)	0.242 7(1.5)
3	0.2035(3)	0.2027(2)	0.200 9 ₄ (0.8)
4	0.1413(3)	0.1404(3)	0.138 6(2.5)
5	0.1279(4)	0.1265(3)	0.123 5(2)
6	0.1023(4)	0.1009(3)	0.097 8(4)
7	0.0965(4)	0.0944(4)	0.089 9(3)
8	0.0828(5)	0.0805(4)	0.075 9(4)
9	0.0800(5)	0.0769(4)	0.071 1(3)
10	0.0716(5)	0.0683(5)	0.062 1(3)
11	0.0707(5)	0.0664(5)	0.058 9(5)
12	0.0651(6)	0.0605(5)	0.052 9(6)
13	0.0654(6)	0.0596(6)	0.050 7(6)
14	0.01617(6)	0.0556(6)	0.046 1(6)
15	0.0630(6)	0.0554(6)	0.044 6(6)
16	0.0606(6)	0.0524(6)	0.040 9(7)
17		0.0528(6)	0.039 6(7)
18		0.0507(6)	0.036 8(9)
19		0.0516(6)	0.035 9(9)
20		0.0501(7)	0.033 5(9)

merical evidence that $C(r)$ approaches zero more slowly than as $1/r$. Finally we show that these finite-system data are consistent with (15), with $\sigma \simeq 0.2$ to 0.3, suggesting that the slower-than- $1/r$ decay indicated by the data is perhaps associated with this logarithmic behavior.

We note that the Heisenberg Hamiltonian $\Delta=1$, $\Gamma=0$ is a very special point: With $\Gamma=0$, for $|\Delta| \leq 1$ there is no LRO, while for $\Delta > 1$ there is LRO. The ground state of the model for $|\Delta| < 1$ is already critical as can be seen from the slow algebraic decay of the correlations. The ground state of the Heisenberg Hamiltonian, therefore, corresponds to a multicritical point in usual finite-temperature critical-phenomena terminology. There are examples of similarly critical models which show logarithmic dependence in the large- r behavior of correlation functions. The q -state Potts model in 2D at its critical temperature is one case: As a function of q , the value $q=4$ is separating second-order from first-order transitions²³ and is also a multicritical point; and further the correlation function for $q=4$ goes as $r^{-1/4}[\ln(r/r_0)]^{-1/8}$.²⁴ Another case is the Kosterlitz-Thouless (KT) model²⁵ where the decay of the correlations is algebraic below T_c and exponential above T_c , while $C(r) \simeq r^{-1/4}[\ln(r/r_0)]^{1/8}$ at T_c .²⁶ So the two can be summarized as $C(r) \simeq r^{-\eta}[\ln(r/r_0)]^\sigma$.²⁷ Furthermore, these two models have an even closer relation to the Heisenberg model. The four-state Potts model actually maps to our Heisenberg model;²⁸ unfortunately the mapping of the correlation function is not known and seems difficult to find. Similarly the KT model is intimately related to the ground state of the 1D quantum sine-Gordon model which maps onto the XXZ model ($\Gamma=0$) ground state with the help of the boson representation.^{20,29} The KT model at T_c corresponds to the Heisenberg model. The correlations showing logarithmic behavior were derived for the above two models using renormalization group techniques.^{24,26}

Now it is generally believed that the *exponent* η found by LP, namely $\eta=1$, is correct. This is because they invoked the exact exponent known from the work of Baxter³⁰ as input to the index relation derived by them. Furthermore the same result was recently derived rigorously by Bogoliubov *et al.* through the quantum inverse scattering method.³¹ Hence it seemed to us plausible to analyze the numerical results in terms of the asymptotic form (15). In the following we will attempt to estimate the parameters in (15) assuming (15) is the true asymptotic form and, in addition, that the larger r 's available are large enough to be in the asymptotic region. In the process we will of course test the consistency of these assumptions with the finite- N results.

First we consider an analysis which does not depend on the extrapolation of $C(r, N)$ to $N \rightarrow \infty$. Consider the structure factor. If we assume (14) and (15), (3) gives³²

$$S(N) \simeq a[\ln(N/2r_0)]^{\sigma+1} + b \quad \text{for } N \rightarrow \infty, \quad (16)$$

$a = 2A/(\sigma+1)$, and b is constant. Then, asymptotically,

$$G(N) = [S(N+2) - S(N)] / [S(N) - S(N-2)] \\ \simeq H(N, \sigma), \quad (17)$$

where

$$H(N, \sigma) = \left\{ \left[\ln \left(\frac{N+2}{2r_0} \right) \right]^{\sigma+1} - \left[\ln \left(\frac{N}{2r_0} \right) \right]^{\sigma+1} \right\} / \left\{ \left[\ln \left(\frac{N}{2r_0} \right) \right]^{\sigma+1} - \left[\ln \left(\frac{N-2}{2r_0} \right) \right]^{\sigma+1} \right\}. \tag{18}$$

To test the relation (17), we define σ_N via $G(N) = H(N, \sigma_N)$, and see if σ_N approaches a limit as N increases for various values of r_0 . The results, based on the values of $S(N)$ in Table IV for $N \leq 24$, are shown in Fig. 9. The errors indicated arise from an assumed error of ± 1 in the last figure of the original data⁷ for $C(r, N)$. Equation (18) implies that σ_N approaches a limit σ as $N \rightarrow \infty$ for any r_0 assumed and with the least N dependence for the correct r_0 . The results are clearly consistent with this; σ_N decreases with N when small r_0 is assumed and it increases when r_0 is large. It apparently converges to $\sigma \cong 0.2$ to 0.3 . The plots with $r_0 \cong 0.6$ to 0.8 give almost flat behavior for $6 \leq N \leq 22$. The extremely slow convergence of σ_N when r_0 is very small or very large, apparent from the figure, is precisely what is expected if the true behavior were

$$S(N) = \bar{a} (\ln N / 2\bar{r}_0)^{\bar{\sigma}+1} + \bar{b}. \tag{19}$$

For if we substitute this into (17) then for $N \rightarrow \infty$ it can be seen that

$$\sigma_N \cong \bar{\sigma} - \bar{\sigma} [\ln(r_0 / \bar{r}_0)] / \ln N.$$

In addition to this slow approach to $\bar{\sigma}$, this gives, for $\bar{\sigma} > 0$, $\delta\sigma_N \cong 0$ when $r_0 \leq \bar{r}_0$, as found in Fig. 9 where $S(N)$

is from the actual chain data. In fact, for $\bar{r}_0 = 0.6$ and $\bar{\sigma} = 0.25$, the plot σ_N versus N for various r_0 looks quantitatively very much like those obtained from actual $S(N)$ as shown in Fig. 9 (with smooth behavior replacing the bumpiness at $N \gtrsim 16$, of course).

Next we plot in Fig. 10, $\ln[r\bar{C}(r)]$ versus $\ln \ln r$, where $\bar{C}(r) = [C(r-1) + 2C(r) + C(r+1)]/4$ is an average introduced to smooth out the even-odd oscillations of $C(r)$. According to (15) this should approach a straight line with slope σ as r increases and $\ln r_0 / \ln r$ becomes negligibly small. A zero slope ($\sigma = 0$) would correspond to the Luther-Peschel result. Clearly a positive slope is observed even at $r < 11$ where the MC results are not essential. And this clearly is strong evidence that the asymptotic decay of $C(r)$ is slower than the $1/r$ LP behavior, quite independent of any assumption as to the form of the asymptotic behavior. Further, the plot indicates consistency with the particular form (15). Assuming that form, we estimated σ and A from the two straight lines shown in the plot. They give $\sigma = 0.21$ and 0.29 and corresponding values $A = 0.53$ and 0.50 . The points from $r \geq 12$ show less scatter from a linear behavior than could be expected from their estimated errors. We think that this is due to one or both of the following: (a) We always chose to err somewhat on the conservative side in deciding the errors, i.e., the errors are overestimated. [Thus

TABLE IV. The structure factor $S(N)$ from Ref. 7 and Eq. (3). Errors are estimated by assuming independent errors of ± 1 in the last figures for original data of $C(r, N)$. Rows 32 and 40 are new MC results, whose errors are estimated from the fluctuations of the MC data for $S(N)$.

N	$S(N)$
4	2.666 67(2)
6	3.109 40(3)
8	3.441 83(4)
10	3.708 54(4)
12	3.931 63(5)
14	4.123 62(5)
16	4.292 31(5)
18	4.442 872(6)
20	4.578 824(6)
22	4.702 912(7)
24	4.817 060(7)
32	5.196(13)
40	5.511(16)

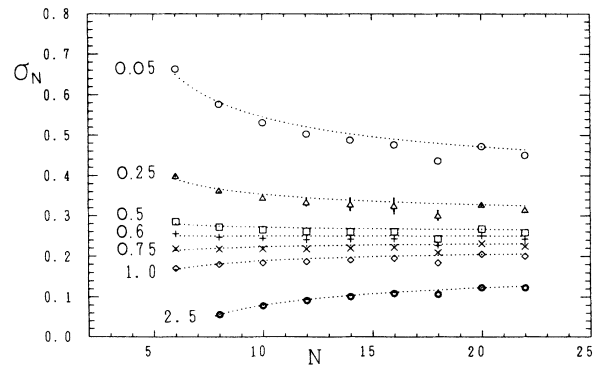


FIG. 9. Exponent σ_N of logarithmic factor [see text following (18)] vs N for various r_0 . Assumed values of r_0 are attached to the plots. Error bars are depicted only for $r_0 = 0.25$ as the data for a same N have the errors with almost same size. Dotted lines show results for the model given by (19) with $\bar{r}_0 = 0.6$ and $\bar{\sigma} = 0.25$.

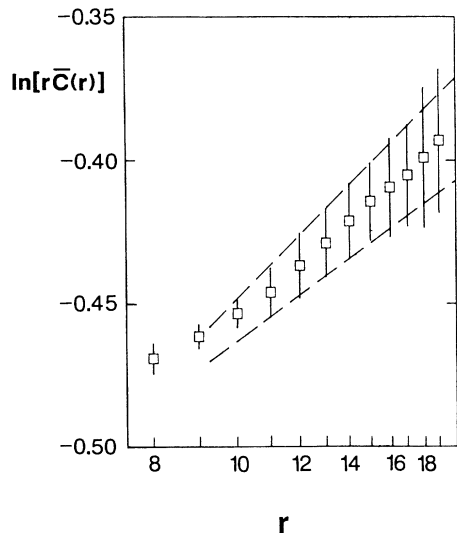


FIG. 10. Plot of $\ln[r\bar{C}(r)]$; the linear scale of the x axis is $\ln \ln r$. The dashed lines correspond to $\sigma=0.29$, $A=0.50$ and $\sigma=0.21$, $A=0.53$, respectively.

the apparent consistency of (15) with the data is stronger than indicated by the errors shown.] (b) The points for large r are correlated because they were obtained from only one ($N=40$) or two ($N=32,40$) rings.

We also plotted $[r\bar{C}(r)]^{1/\sigma}$ versus $\ln r$ for various assumed σ to see the linearity of the plot. The linearity in fact does not depend very much on σ . We show the plot with $\sigma=0.25$ in Fig. 11. The least-square fit assuming linear dependence between $r=9$ and 19 gives $A=0.50$ and $r_0=0.75$ consistent with the previous analysis of S_N . The fitted value of A does not depend much on the assumed σ and changes from 0.55 to 0.45 while r_0 decreases from 1.3 to 0.44 with σ varying from 0.2 to 0.3. The last test we consider is based on an examination of

$$K(N) = (N/2)\bar{C}(N/2, N)$$

[note: $C(N/2+1, N) = C(N/2-1, N)$]. If we assume (14) and (15), it follows³¹ that

$$K(N) \sim Af\left(\frac{1}{2}\right) \left[\ln \left[\frac{N}{2r_0} \right] \right]^\sigma$$

TABLE V. The slope of $\ln(N/2)C(N/2, N) = \ln K(N)$ vs $\ln \ln(N/2)$, obtained from the least-square fits of three points (four points for the last column).

$N/2$	5-7	6-8	7-9	8-10	9-11	10-12	12-16	12-20
Slope of $\ln k(N)$	0.134	0.140	0.171	0.176	0.194	0.199	0.19±0.10	0.26±0.07

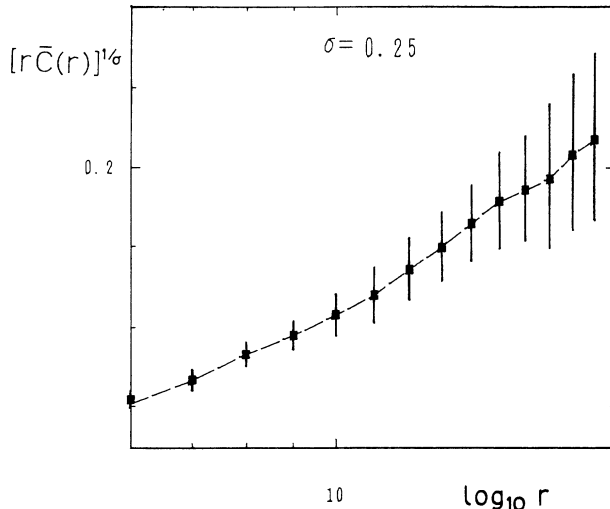


FIG. 11. Plot of $[r\bar{C}(r)]^{1/\sigma}$ for $\sigma=0.25$; the linear scale of the x axis is $\ln r$.

for $N \rightarrow \infty$. The slope of $\ln K(N)$ versus $\ln \ln N/2$ should thus approach σ for large N . As seen from Table V, it is still increasing with slight oscillations in the region considered, and it is plausible to expect that it will approach a value consistent with that of σ obtained previously.

VIII. SUMMARY AND DISCUSSION

We have presented a novel Monte Carlo simulation of the spin correlations in the ground state of the spin- $\frac{1}{2}$ Heisenberg chain which is based on the Sutherland mapping between the spin-chain ground state and the six-vertex model at its critical temperature. The new results are for chains with number of spins $N=32$ and 40. We have given evidence which suggests that the asymptotic decay of the spin-correlation function is slower than the $1/r$ behavior of Luther and Peschel, and that this might be attributed to a logarithmic factor, i.e., $C(r) \sim A(1/r)[\ln(r/r_0)]^\sigma$. The evidence consists of a plausibility argument (based on known behavior of related models) for this form, plus analysis of data for finite chains of up to 40 spins, assuming such a form, and assuming that the larger r 's available are in the asymptotic region. On the basis of the four rather different analyses presented, we conclude that $0.2 \lesssim \sigma \lesssim 0.3$.

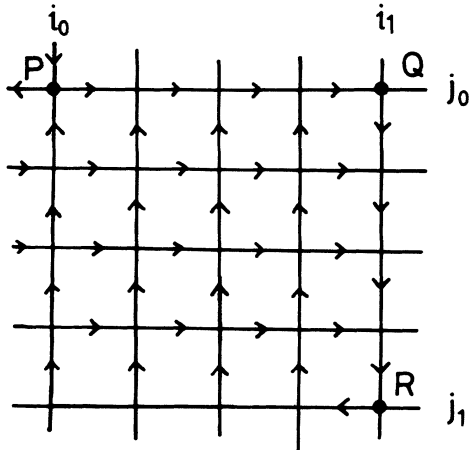


FIG. 12. A configuration of the six-vertex model which accompanies with a vertex of type f at P . Definitions of Q and R are in the text.

ACKNOWLEDGMENTS

We acknowledge helpful discussions with S. D. Mahanti, R. Day, M. Challa, J. Bass, D. Scalapino, V. Emery, M. P. M. den Nijs, F. D. M. Haldane, S. Takada, K. Saitoh, and M. Fisher. One of us (K.K.) would like to thank the members of the Department of Physics, MSU, for their hospitality.

APPENDIX

In this appendix we prove that for the six-vertex model MLF's on all possible squares connect all the configurations in a subspace with a given Σ and Π if $\Sigma \neq \pm N$ and $\Pi \neq \pm M$. For the proof we show that any configuration can be changed to the configuration $C_0(\Sigma, \Pi)$ where $\sigma_{ij} = 1$ for $1 \leq i \leq (\Sigma + N)/2$ and any j and $\tau_{ij} = 1$ for $1 \leq j \leq (\Pi + M)/2$ and any i by successive operations of MLF's. Then $C_0(\Sigma, \Pi)$ can be changed to any other configuration because the inverse of any allowed change is also allowed. This completes the proof. We show (i) any configuration can be changed by MLF's to a configuration in which only vertices of type $a-d$ appear, i.e., a configuration whose columns and rows have arrows pointed in the same direction (let us call such a configuration a straight configuration), and (ii) any

straight configuration can be changed to $C_0(\Sigma, \Pi)$.

Proof of (i). Let us assume that the columns 1 to $i_0 - 1$ are straight and the column i_0 is not. Let the vertex (i_0, j_0) be of type f (P in Fig. 12). Let (i_1, j_0) (Q in Fig. 12) be the first vertex with a downward arrow starting from it when we proceed from P to the right on the row j_0 ($i_0 < i_1 \leq N$). Next we follow downward arrows starting from Q to $R = (i_1, j_1)$ where a leftward arrow starts for the first time. Then we easily see that $\sigma_{ij} = 1$ for $i_0 \leq i \leq i_1 - 1$ and $j_1 \leq j \leq j_0 - 1$ and also $\tau_{ij} = 1$ for $i_0 \leq i \leq i_1 - 1$ and $j_1 + 1 \leq j \leq j_0$ are forced (see Fig. 12). An MLF is possible on the square sharing R as its lower-right corner. Successive operations of MLF on squares lying between columns $i_1 - 1$ and i_1 change $\sigma_{i_1 - 1, j}$ for $j_1 \leq j \leq j_0 - 1$ to -1 . Then we search for $R' = (i_1 - 1, j'_1)$ on the column $i_1 - 1$ where a leftward arrow between columns $i_1 - 2$ and $i_1 - 1$ starts for the first time [$j'_1 - j_1 \leq 0 \text{ Mod}(M)$] and operate MLF's on the squares between columns $i_1 - 2$ and $i_1 - 1$ as before. Such j'_1 is always found, since $\sigma_{i_1 - 1, j_0} = 1$ and therefore there must be at least one vertex of type f on the column $i_1 - 1$. Repeating this process on the squares between columns $i_1 - 2$ and i_0 we finally change $\sigma_{i_0, j}$ for $j_2 \leq j \leq j_0 - 1$ to -1 ($j_2 \leq j_1$). Repetition of this process makes the column i_0 straight and successively all columns can be made straight.

Proof of (ii). It is sufficient to show that directions of two neighboring straight columns (rows) can be exchanged. Let us assume the column i is upward and $i + 1$ downward. There must be a leftward row j_0 with the row $j_0 + 1 \text{ [Mod}(M)]$ rightward due to the assumption $\Pi \neq \pm M$. Then MLF is possible on the square sharing the vertex (i, j_0) as its lower-left corner and it exchanges σ_{ij_0} and σ_{i+1, j_0} . If the row $j_0 + 2$ is rightward again we can do an MLF on the neighboring square proceeding upward exchanging $\sigma_{i, j_0 + 1}$ and $\sigma_{i+1, j_0 + 1}$. We can proceed upward until we encounter a leftward row. Let the row j_1 be the lowest leftward row with $j_1 > j_0$ and j_2 the lowest rightward row with $j_2 > j_1$. Then we can do MLF's on the squares between these rows starting from the uppermost one and proceeding downwards and exchange σ_{ij} and $\sigma_{i+1, j}$ for $j_1 \leq j \leq j_2 - 1$. Repetition of this process exchanges σ_{ij} and $\sigma_{i+1, j}$ for all j . Exchange of rows can be done in the same way under the assumption $\Sigma \neq \pm N$.

*Permanent address: Institute of Physics, University of Tsukuba, Ibaraki 305, Japan.

¹For review, see J. C. Bonner, H. W. Blöte, H. Beck, and G. Müller, in *Physics in One Dimension*, edited by J. Bernasconi and T. Schneider (Springer, Berlin, 1981), p. 115.

²F. D. M. Haldane, Phys. Rev. Lett. **50**, 1153 (1983); Phys. Lett. **93A**, 464 (1983).

³H. Bethe, Z. Phys. **71**, 205 (1931); L. Hulthen, Ark. Mat. Astron. Fyz. **26A**(11), 1 (1938); C. N. Yang and C. P. Yang, Phys.

Rev. **150**, 321 (1966); **150**, 327 (1966); **151**, 258 (1966); J. des Cloizeaux and M. Gaudin, J. Math. Phys. **7**, 1384 (1966).

⁴L. Takhtajan, Phys. Lett. **87A**, 479 (1982); H. M. Babujian, *ibid.* **90A**, 205 (1982).

⁵A. Luther and I. Peschel, Phys. Rev. B **12**, 3908 (1975).

⁶F. D. M. Haldane, Phys. Rev. Lett. **45**, 1358 (1980).

⁷J. C. Bonner and M. E. Fisher, Phys. Rev. **135**, A640 (1964); W. Grieger, Phys. Rev. B **30**, 344 (1984); J. Borysowicz, T. A. Kaplan, and P. Horsch, *ibid.* **31**, 1590 (1985); H. Betsuyaku

- and T. Yokota, *ibid.* **33**, 6505 (1986); E. R. Gagliano, E. Dagotto, A. Moreo, and F. C. Alcaraz, *ibid.* **34**, 1677 (1986); **35**, 5297(E) (1987).
- ⁸R. Jullien and P. Pfeuty, *J. Phys. A* **14**, 3111 (1981); R. Botet and R. Jullien, *Phys. Rev. B* **27**, 613 (1983); U. Glaus and T. Schneider, *ibid.* **30**, 215 (1984); T. A. Kaplan, P. Horsch, and J. Borysowicz, *ibid.* **35**, 1877 (1987).
- ⁹A. A. Belavin, A. M. Polyakov, and A. B. Zamolodchikov, *Nucl. Phys.* **B241**, 186 (1984); J. L. Cardy, *J. Phys. A* **17**, L385 (1983); **19**, L1093 (1986); *Nucl. Phys.* **B270**, 186 (1984); H. J. Shulz and T. Ziman, *Phys. Rev. B* **33**, 6545 (1986); H. Blöte, J. L. Cardy, and M. P. Nightingale, *Phys. Rev. Lett.* **56**, 742 (1986).
- ¹⁰K. Kubo and S. Takada, *J. Phys. Soc. Jpn.* **55**, 438 (1986); S. Takada and K. Kubo, *ibid.* **55**, 1671 (1986); K. Saitoh, S. Takada, and K. Kubo, *ibid.* **56**, 3755 (1987).
- ¹¹For a review, see M. Suzuki, in *Quantum Monte Carlo Methods in Equilibrium and Nonequilibrium Systems*, edited by M. Suzuki (Springer, Berlin, 1987), p. 2.
- ¹²B. Sutherland, *J. Math. Phys.* **11**, 3183 (1970).
- ¹³T. A. Kaplan and Kenn Kubo, *Bull. Am. Phys. Soc.* **32**, 777 (1987).
- ¹⁴J. R. Borysowicz, A. Moreo, T. A. Kaplan, and K. Kubo, *Nucl. Phys.* **B300**[FS22], 301 (1988).
- ¹⁵M. H. Kalos, *Phys. Rev.* **128**, 1791 (1962).
- ¹⁶E. Hirsch, R. L. Sugar, D. J. Scalapino, and R. Blankenbecler, *Phys. Rev. B* **26**, 5033 (1982); H. de Raedt and A. Lagendijk, *Phys. Rev. Lett.* **49**, 1522 (1982).
- ¹⁷J. J. Cullen and D. P. Landau, *Phys. Rev. B* **27**, 297 (1983).
- ¹⁸W. Marshall, *Proc. R. Soc. London, Ser. A* **232**, 48 (1955).
- ¹⁹ $C(2, \infty) = 0.242719$ was found by M. Takahashi, *J. Phys. C* **10**, 1289 (1977).
- ²⁰M. P. M. den Nijs, *Phys. Rev. B* **23**, 6111 (1981).
- ²¹In Ref. 7 (J. Borysowicz *et al.*), the possibility of logarithmic corrections was considered. However, this was based on explicit assumptions behind extrapolation of the *chain* data, assumptions that were found to be violated when a larger- N chain was calculated ($N = 18$). Conclusions and speculations based on extrapolation from the chain data in that work are no longer considered viable.
- ²²D. J. Scalapino, V. J. Emery, M. P. M. den Nijs, and I. Affleck (private communication).
- ²³R. J. Baxter, *J. Phys. C* **6**, L445 (1973).
- ²⁴J. L. Cardy, M. Nauenberg, and D. J. Scalapino, *Phys. Rev. B* **22**, 2560 (1980).
- ²⁵J. M. Kosterlitz and D. J. Thouless, *J. Phys. C* **6**, 1181 (1973).
- ²⁶J. M. Kosterlitz, *J. Phys. C* **7**, 1046 (1974).
- ²⁷*Additive* logarithmic corrections in the system size to the ground-state energy of the antiferromagnetic Heisenberg ring were derived by T. Woynarovich and H. P. Eckle, *J. Phys. A* **20**, L97 (1987). Their claim that extrapolations from small N for the $S = \frac{1}{2}$ Heisenberg model are misleading is not justified for $C(r, N)$. *Prima facie* evidence for this statement is the success of Bonner and Fisher's extrapolation of $C(1, N)$ and $C(N/2, N)$ (Ref. 7) and the extrapolation of $C(2, N)$ (see Kaplan *et al.*, Ref. 8). Furthermore, we have found that polynomial extrapolation of $C(1, N)$ not only does not fail using even very large N , but in fact is very useful.
- ²⁸R. J. Baxter, S. B. Kelland, and F. Y. Wu, *J. Phys. A* **9**, 397 (1976).
- ²⁹S. T. Chui and P. A. Lee, *Phys. Rev. Lett.* **35**, 315 (1975). See also V. J. Emery, in *Highly Conducting One-Dimensional Solids*, edited by J. T. Devreese (Plenum, New York, 1979).
- ³⁰R. J. Baxter, *Phys. Lett.* **26**, 834 (1971); *Ann. Phys. (N.Y.)* **70**, 193 (1972).
- ³¹N. M. Bogoliubov, A. G. Izergin, and V. E. Korepin, *Nucl. Phys.* **B275**[FS17], 687 (1986).
- ³²The scaling assumption (14) and the asymptotic behavior (15) lead to (16), and the asymptotic behavior of $K(N)$ which is defined later. The scaling assumption is not necessary, and weaker assumptions about finite-size effects for $C(r, N)$ could lead to the same asymptotic behavior of $S(N)$ and $K(N)$.